Laser frequency combs and ultracold neutrons to probe braneworlds through induced matter swapping between branes

Sarrazin, Michael; Petit, F.

Link to publication

Laser frequency combs and ultracold neutrons to probe braneworlds through induced matter swapping between branes

Michaël Sarrazin[1, *] and Fabrice Petit[2, †]

¹Department of Physics,
University of Namur (FUNDP),
61 rue de Bruxelles, B-5000 Namur, Belgium
²Belgian Ceramic Research Centre,
4 avenue du gouverneur Cornez, B-7000 Mons, Belgium

This paper investigates a new experimental framework to test the braneworld hypothesis. Recent theoretical results have shown the possibility of matter exchange between branes under the influence of suitable magnetic vector potentials. It is shown that the required conditions might be achieved with present-day technology. The experiment uses a source of pulsed and coherent electromagnetic radiation and relies on the Hänsch frequency comb technique well-known in ultrahigh-precision spectroscopy. A good matter candidate for testing the hypothesis is a polarized ultracold neutron gas for which the number of swapped neutrons is measured.

PACS numbers: 11.25.Wx, 12.60.-i, 13.40.-f, 14.20.Dh

I. INTRODUCTION

Over the last two decades, the concept of a braneworld universe has gained a growing importance in theoretical physics. The braneworld hypothesis assumes that our Universe is just a membrane (a brane) embedded in a larger dimensional manifold (a bulk) having $N > 4$ dimensions [1–4]. Standard model particles are expected to stay confined in our brane while the other branes are normally considered invisible to us. A wealth of papers have demonstrated that this geometrical approach offers nice explanations for several physical phenomena like the dark matter origin [3] or the hierarchy between the electroweak and Planck scales [4] for instance. As a consequence, finding evidence of the existence of branes or extra dimensions is a major challenge for the twenty-first century. Experimental results could arise from high energy physics (observation of Kaluza-Klein tower states [5] for instance) or low energy physics (deviations from the inverse square law of gravity [6] for instance). In the present paper, we are mainly motivated by a low energy approach and we explore how the quantum dynamics of fermions is modified at a nonrelativistic energy scale when the higher dimensional bulk contains more than only one brane.

In a previous work [7], it has been shown that for a bulk containing at least two branes, matter swapping between these two worlds might be possible (although the effect would remain difficult to observe). In some conditions, this matter exchange could be triggered by using suitable magnetic vector potentials [7–9]. This effect was studied through a quantum description of spin-½ fermions in a $M_4 \times Z_2$ universe, which is a model-independent low energy limit of some two-brane world theories of the Universe [7]. However, the situations considered in previous papers were rather simplistic [7–9]. In the present work, we investigate further this effect by reconsidering it from a more realistic experimental point of view. To that end, a simple and inexpensive experimental setup is proposed, inspired from designs used in neutron physics investigations [10–13] and in spectroscopy [14–17].

In section II, the mathematical and physical assumptions underlying the low energy description of spin-½ fermions in a two-brane world are reviewed. The theoretical conditions of matter swapping between branes are given in section III. We discuss the environmental conditions that could preclude the swapping to occur. The role of the magnetic vector potentials, which are required to match the conditions of successful matter exchange between branes is also discussed. Finally, in section IV an experimental setup which might be used to confirm our theoretical prediction is described. The proposed experiment relies on the use of a polarized ultracold neutron gas [10–13] and coherent electromagnetic radiation thanks to a Hänsch frequency comblike technique [14–17]. It is demonstrated that for certain experimental parameters, the conditions of a resonant matter exchange between branes may be obtained.

*Electronic address: michael.sarrazin@fundp.ac.be
†Electronic address: f.petit@bcrc.be

II.   MODEL OF THE LOW ENERGY LIMIT OF TWO-BRANE WORLDS

In a recent work [7], regarding the dynamics of spin-$1/2$ particles, it has been demonstrated that at low energies any two-brane world related to a domain wall approach can be described by a simple noncommutative two-sheeted spacetime $M_4 \times Z_2$. For instance, a two-brane world made of two domain walls on a continuous $M_4 \times R_1$ manifold is well modeled by a discrete product space $M_4 \times Z_2$ at low energies. The continuous real extra dimension R_1 is replaced by an effective phenomenological discrete two-point space Z_2. At each point along the discrete extra dimension Z_2 there is then a four-dimensional spacetime M_4 endowed with its own metric field. Both branes/sheets are then separated by a phenomenological distance δ which is inversely proportional to the overlap integral of the extra-dimensional fermionic wave functions of each brane over the fifth dimension R_1 [7]. Considering the electromagnetic gauge field, it has been also demonstrated that the five-dimensional $U(1)$ bulk gauge field [18] is substituted by an effective $U(1) \otimes U(1)$ gauge field acting in the $M_4 \times Z_2$ spacetime.

It is important to stress that the equivalence between the continuous two-domain wall approaches and the noncommutative two-sheeted spacetime model is rather general and does not rely for instance on the domain walls features or on the bulk dimensionality [7]. It allows us to conjecture that at low energy, regarding the quantum dynamics of fermions, any multidimensional setup containing two branes can be described by a two-sheeted spacetime in the formalism of noncommutative geometry. Since this matter has already been considered in detail in a previous work [7], in the following, we are only considering the relevant $M_4 \times Z_2$ limit.

The mathematical description of fermions in the noncommutative two-sheeted spacetime is mainly based on the works of Connes *et al* [19] and relies on the definition of a noncommutative exterior derivative D acting in $M_4 \times Z_2$. Because of the specific geometrical structure of the bulk, this operator is given by [7–9]:

$$D_\mu = \begin{pmatrix} \partial_\mu & 0 \\ 0 & \partial_\mu \end{pmatrix} \text{ and } D_5 = \begin{pmatrix} 0 & g \\ -g & 0 \end{pmatrix} \tag{1}$$

with $\mu = 0, 1, 2, 3$ and where the term $g = 1/\delta$ acts as a finite difference operator along the discrete dimension. g also appears as a coupling strength, which describes the interaction between the branes. Although g is a parameter, which results from the exact and complex brane characteristics, it can be resolute from experiment. One is able to build the Dirac operator defined as $\slashed{D} = \Gamma^N D_N = \Gamma^\mu D_\mu + \Gamma^5 D_5$ by considering the following extension of the gamma matrices (we are working in the Hilbert space of spinors [19]): $\Gamma^\mu = \mathbf{1}_{2\times 2} \otimes \gamma^\mu$ and $\Gamma^5 = \sigma_3 \otimes \gamma^5$, where γ^μ and $\gamma^5 = i\gamma^0 \gamma^1 \gamma^2 \gamma^3$ are the usual Dirac matrices and σ_k $(k = 1, 2, 3)$ the Pauli matrices. By introducing a general mass term M, a two-brane Dirac equation is then derived [7]:

$$\begin{aligned} \slashed{D}_{dirac}\Psi &= \left(i\slashed{D} - M \right)\Psi = \left(i\Gamma^N D_N - M \right)\Psi = \\ &= \begin{pmatrix} i\gamma^\mu \partial_\mu - m & ig\gamma^5 - m_c \\ ig\gamma^5 - m_c^* & i\gamma^\mu \partial_\mu - m \end{pmatrix} \begin{pmatrix} \psi_+ \\ \psi_- \end{pmatrix} = 0 \end{aligned} \tag{2}$$

where "$*$" denotes the complex conjugate. The off-diagonal mass term m_c can be justified from a two-brane(-domain wall) structure of the Universe [7]. It can be noticed that by virtue of the two-sheeted structure of spacetime, the wave function ψ of the fermion is split into two components, each component living on a distinct spacetime sheet (i.e. brane). In this notation, the indices "$+$" and "$-$" allow us to discriminate between the two branes. If one considers the $(+)$ sheet as our own brane, then the $(-)$ sheet can be considered as a hidden brane.

A.   Electromagnetic gauge field

As explained in the introduction, we want to show how the electromagnetic field influences the dynamics of fermions. The reason for the electromagnetic force, in contrast to the electroweak or strong force, rests on the choice of a simple gauge group and just serves our experimental purpose. Incorporating the electromagnetic field $\slashed{A}$ in the model $(\slashed{D}_A \rightarrow \slashed{D} + \slashed{A})$ [7–9], the usual $U(1)$ gauge field must be substituted by an extended $U(1) \otimes U(1)$ gauge field accounting for the two-brane structure [7]. The group representation is therefore $G = diag(\exp(-iq\Lambda_+), \exp(-iq\Lambda_-))$. According to the gauge transformation rule: $\slashed{A}' = G\slashed{A}G^\dagger - iG\left[\slashed{D}_{dirac}, G^\dagger\right]$, the appropriate gauge field is given by (see Ref. [7])

$$\slashed{A} = \begin{pmatrix} iq\gamma^\mu A_\mu^+ & \gamma^5 \chi \\ \gamma^5 \overline{\chi} & iq\gamma^\mu A_\mu^- \end{pmatrix} \text{ with } \chi = \varphi + \gamma^5 \phi \tag{3}$$

where φ and ϕ are the scalar components of the field χ and $\overline{\chi} = \gamma^0 \chi^\dagger \gamma^0$. If χ is different from zero, each charged particle of each brane becomes sensitive to the electromagnetic fields of both branes irrespective of their localization

in the bulk. This kind of exotic interaction has been considered previously in literature within the framework of the mirror matter paradigm [20] and is not covered by the present paper. Moreover, to be consistent with known physics, at least at low energies, χ is necessarily tiny (whereas $qA_\mu^\pm$ need not to be). This is theoretically corroborated by the gauge transformation rule which shows that during each gauge transformation, $|\varphi|$ (respectively $|\phi|$) varies with an amplitude of order g (respectively $|m_c|$) whatever Λ_+ and Λ_-. Using the covariant derivative $\slashed{D}_A \to \slashed{D} + \slashed{A}$ and according to expression (3), the electromagnetic field can be easily introduced in the two-brane Dirac equation (Eq. (2)). Then, we get:

$$
\begin{aligned}
\left(i\slashed{D}_A - M\right)\Psi &= 0 \\
&= \begin{pmatrix} i\gamma^\mu(\partial_\mu + iqA_\mu^+) - m & i\widetilde{g}\gamma^5 - \widetilde{m}_c \\ i\widetilde{g}^*\gamma^5 - \widetilde{m}_c^* & i\gamma^\mu(\partial_\mu + iqA_\mu^-) - m \end{pmatrix}\begin{pmatrix} \psi_+ \\ \psi_- \end{pmatrix} = 0
\end{aligned}
\tag{4}
$$

with $\widetilde{g} = g + \varphi$ and $\widetilde{m}_c = m_c - i\phi$. It is important to underline that the field χ just leads to replacing g and m_c by the effective parameters $\widetilde{g}$ and $\widetilde{m}_c$. In the following, we assume that $\widetilde{g} \approx g$ and $\widetilde{m}_c \approx m_c$ since $|\varphi|$ (respectively $|\phi|$) should not exceed the amplitude of g (respectively $|m_c|$). This choice allows a further simplification of the model. It is somewhat equivalent to set the off-diagonal term χ to zero. With such a choice, we simply assume that the electromagnetic field of a brane couples only with the particles belonging to the same brane. Each brane possesses its own current and charge density distribution as sources of the local electromagnetic fields. On the two branes live then the distinct A_μ^+ and A_μ^- electromagnetic fields. The photon fields $A_\mu^\pm$ behave independently of each other and are totally trapped in their original brane in accordance with observations: photons belonging to a given brane are not able to reach the other brane. As a noticeable consequence, the structures belonging to the branes are mutually invisible by local observers.

B.   Nonrelativistic limit and phenomenology

As explained in the introduction, we are concerned about phenomena occurring at the nonrelativistic energy scale. In Refs. [8], it was indeed demonstrated that any relativistic particle is trapped in its own brane. As a consequence, the model predicts that there is no hope to observe the exchange of standard model particles between branes for relativistic energies − a conclusion that contrasts with the usual belief on the energy scales at which extra dimensions' effects should become noticeable. This is the reason why this paper is restricted to the case of nonrelativistic particles only.

Let us derive the nonrelativistic limit of the two-brane Dirac equation (4). Following the well-known standard procedure, a two-brane Pauli equation can be derived:

$$
i\hbar\frac{\partial}{\partial t}\begin{pmatrix} \psi_+ \\ \psi_- \end{pmatrix} = \{\mathbf{H}_0 + \mathbf{H}_{cm} + \mathbf{H}_c\}\begin{pmatrix} \psi_+ \\ \psi_- \end{pmatrix}
\tag{5}
$$

where ψ_+ and ψ_- correspond to the wave functions in the $(+)$ and $(-)$ branes respectively. ψ_+ and ψ_- are here Pauli spinors. The Hamiltonian $\mathbf{H}_0$ is a block-diagonal matrix where each block is simply the classical Pauli Hamiltonian expressed in each brane:

$$
\mathbf{H}_\pm = -\frac{\hbar^2}{2m}\left(\nabla - i\frac{q}{\hbar}\mathbf{A}_\pm\right)^2 + g_s\mu\frac{1}{2}\sigma\cdot\mathbf{B}_\pm + V_\pm
\tag{6}
$$

such that $\mathbf{A}_+$ and $\mathbf{A}_-$ correspond to the magnetic vector potentials in the branes $(+)$ and $(-)$ respectively. The same convention is applied to the magnetic fields $\mathbf{B}_\pm$ and to the potentials $V_\pm$. $g_s\mu$ is the magnetic moment of the particle with g_s the gyromagnetic factor and μ the magneton. In addition to these "classical" terms, the two-brane Hamiltonian comprises also new terms specific to the two-brane world:

$$
\mathbf{H}_c = \begin{pmatrix} 0 & m_c c^2 \\ m_c^* c^2 & 0 \end{pmatrix}
\tag{7}
$$

and

$$
\mathbf{H}_{cm} = -igg_s\mu\frac{1}{2}\begin{pmatrix} 0 & \sigma\cdot\{\mathbf{A}_+ - \mathbf{A}_-\} \\ -\sigma\cdot\{\mathbf{A}_+ - \mathbf{A}_-\} & 0 \end{pmatrix}
\tag{8}
$$

$\mathbf{H}_c$ is responsible for free spontaneous oscillations of fermions between each brane. Nevertheless, as mentioned in Refs. [7, 9], these oscillations are expected to be hardly observable due to environmental effects which freeze the oscillations (see also section III A). As a consequence, $\mathbf{H}_c$ will be neglected in the following [7]. By contrast $\mathbf{H}_{cm}$ is a
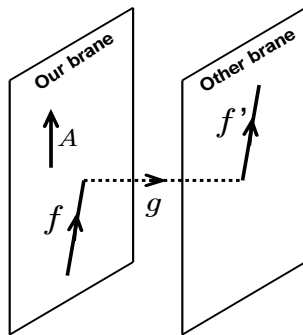
FIG. 1: Naive view of the induced transfer of a fermion (a neutron for instance) between two branes. The fermion f in our brane is transferred to another brane (fermion f') under the influence of a suitable magnetic vector potential $\mathbf{A}$. g represents the coupling constant between branes.

geometrical coupling involving the gauge fields of the two branes. It is worth noticing that this coupling term depends on the magnetic moment and on the difference between the local (i.e. on a brane) values of the magnetic vector potentials (see Refs. [7–9] for more details and discussions). The coupling term $\mathbf{H}_{cm}$ implies that matter exchange should be possible between the branes. Its form suggests that particles could experience Rabi-like oscillations between the branes that might be triggered by suitable magnetic vector potentials (see Fig. 1).

III. RESONANT MATTER OSCILLATIONS BETWEEN BRANES

We consider the possibility of a matter exchange (or swapping) between two branes through an idealized case and from equations (5) to (8). Moreover, $\mathbf{H}_c$ is neglected relative to $\mathbf{H}_{cm}$. Let us consider a neutral particle ($q = 0$) endowed with a magnetic moment (a neutron for instance), initially ($t = 0$) localized in our brane in a region of curlless rotating magnetic vector potential such that $\mathbf{A}_+ = \mathbf{A}_p = A_p \mathbf{e}(t)$ and $\mathbf{A}_- = 0$, with $\mathbf{e}(t) = (\cos \omega t, \sin \omega t, 0)$. ω is the angular frequency of the field $\mathbf{A}_+$, which can be null ($\omega = 0$) in the static field case. Assuming that the conventional part of the Pauli Hamiltonian $\mathbf{H}_\pm$ can be written as $\mathbf{H}_\pm = V_\pm$, any particle initially in a spin-down state for instance (according to $\mathbf{e}_3 = \mathbf{e}_z = (0, 0, 1)$) and localized in our brane at $t = 0$ can be detected in the second brane at time t according to the probability [9]:

$$P(t) = \frac{4\Omega_p^2}{(\eta - \omega)^2 + 4\Omega_p^2} \sin^2 \left((1/2)\sqrt{(\eta - \omega)^2 + 4\Omega_p^2} t \right) \tag{9}$$

where $\Omega_p = g g_s \mu A_p / (2\hbar)$ and $\eta = (V_+ - V_-)/\hbar$. In addition, in the second brane, the particle is then in a spin-up state. $\eta \hbar$ is an effective potential that sums up all the interactions between the particle and its environment described by $\mathbf{H}_\pm$. Those environmental effects are discussed in section III A. Eq. (9) shows how the particle is transferred to the other brane through a process involving Rabi-like oscillations. Eq. (9) shows that a resonant exchange occurs whenever the magnetic vector potential rotates with an angular frequency $\omega = \eta$. A similar expression is obtained by applying the substitution $\omega \to -\omega$ if the particle is in a spin-up state at $t = 0$ (the resonance is then achieved with a counterrotative vector potential). In this case, the particle is in a spin-down state in the second brane after exchange. Note that Eq. (9) corresponds to a resonant process with a half-height width $\Delta \omega = 4\Omega_p$. The weaker the coupling constant g is, the narrower the resonance is. By contrast, the greater A_p is, the broader the resonance is.

Of course when $\omega \neq \eta$, or even in the static field case ($\omega = 0$), matter oscillations between branes occurs as well. Nevertheless, due to environmental effects discussed in section III A, the amplitude of these oscillations must probably be strongly damped and hardly observable.

It is clear that the situation described by Eq. (9) remains rather simplistic. In the suggested experiment (section IV) we will propose a more realistic situation to achieve resonant matter exchange through the use of coherent electromagnetic radiations.

A.   Freezing oscillations and environmental effective potential η

As detailed in previous papers [8, 9], usual environmental interactions are strong enough to suppress matter oscillations between adjacent branes. This can be easily checked by considering Eq. (9) showing that if $\omega \neq \eta$ then $P(t)$ decreases as η increases in comparison to Ω_p. Based on the fact that no such oscillations have been observed so far, we can expect that the ratio Ω_p/η is usually very small. Therefore, any experiment seeking for such oscillations should focus on the quest of resonant responses (i.e. when $\omega = \eta$) in order to avoid the environmental confinement.

Next, if one considers an experiment involving a set of particles with strong collisional dynamics, any coherent oscillatory behavior would probably be inhibited. From the point of view of a single particle, each collision resets the probability of transfer according to a quantum Zeno-like effect. This oscillation damping is also expected to increase dramatically with temperature.

Note that the same environmental effects are responsible for the negligible role of $\mathbf{H}_c$, which cannot be artificially enhanced by contrast to $\mathbf{H}_{cm}$.

Therefore a prerequisite for observing the oscillatory behavior of the particles between branes is to keep each particle isolated from the environment as much as possible and to apply very specific magnetic vector potentials, i.e. a context never met in any kind of experiments so far.

As a consequence, it seems natural to work preferentially with ultracold neutrons [10–13], which are insensitive to electric fields. In addition, neutron magnetic sensibility is the result of its magnetic moment only. Therefore, convenient Helmholtz coils should be used to cancel the ambient magnetic fields (such as the Earth's). Ambient electromagnetic waves could be cancelled too in a large spectral frequency domain by working with a cooled setup (to avoid black body emissions) and using a combination of convenient shields, such as the Faraday cage and lead brick walls. Moreover, one may assume that by using a low-density neutron gas the collisions between particles should be prevented. Of course, such an experimental setup should be emptied of atmospheric gases.

At last, note that for a neutron shielded from magnetic fields, $\eta = (V_{grav,+} - V_{grav,-})/\hbar$ (i.e. only gravitational contributions are considered). However, it is difficult to assess the value of $\eta\hbar$. For instance, the estimations given in Ref. [9] suggest that $V_{grav,+}$ could be of the order of -500 eV owing to the Milky Way core gravitational influence exerted on neutrons. By contrast, the Sun, the Earth and the Moon lead respectively to contributions of about -9 eV, -0.65 eV and -0.1 meV. Nevertheless, since the gravitational contribution of the other brane ($V_{grav,-}$) remains unknown, η appears therefore as an effective unknown parameter (which can be either positive or negative) of the model. In addition, η might be also time-dependent. It is instructive for instance to consider the motion of Earth around the Sun. From the aphelion to the perihelion, the gravitational energy (due to the Sun) of a neutron varies from -9.12 eV to -9.43 eV leading then to an absolute shift of η of about 1.7 meV/day. The time dependence of η could have several different origins such as the relative particle motion with reference to the unknown mass distribution in the second brane for instance. It is therefore impossible to theoretically assess the time rate of shift of η even if this value is expected to be very small. As a consequence, the unknown magnitude and time dependence of η are among the main difficulties in the search for resonant matter swapping between branes.

B.   Magnetic vector potential: Ambient and artificial contributions

Before detailing a suitable experimental setup, we first need to address the issue of a hypothetical ambient magnetic vector potential. The existence of such a potential was recently debated in literature in the context of photon mass measurement [21]. For instance, in Refs. [21], ambient magnetic vector potential was estimated by integrating $\mathbf{B}_{amb} = \nabla \times \mathbf{A}_{amb}$ and considering ambient magnetic fields $\mathbf{B}_{amb}$. It was demonstrating that $A_{amb} = RB_{amb}$, where R is the typical distance from sources. From earth magnetic field measurements, it was therefore assessed there is an ambient contribution A_{amb} of about 200 T·m whereas from the Coma galactic cluster magnetic field, a value of $A_{amb} \sim 10^{12}$ T·m was calculated. Although these assessments do not really constrain the present model, they raise a number of questions. Indeed, several authors have pointed out that any assessment of the ambient magnetic vector potential from such simple calculations was unreliable (see Luo *et al* [21]). The magnetic vector potential derived that way is the transversal contribution only whereas any vector potential comprises three parts: $\mathbf{A}_{amb} = \mathbf{A}_\perp + \mathbf{A}_\parallel + \mathbf{A}_{cte}$. Here $\mathbf{A}_\perp$ is the transverse part such that $\mathbf{B}_{amb} = \nabla \times \mathbf{A}_\perp$, $\mathbf{A}_\parallel$ is the longitudinal component such that $\nabla \times \mathbf{A}_\parallel = \mathbf{0}$, and $\mathbf{A}_{cte}$ is a constant vector. It is obvious that a rigorous assessment of the ambient magnetic vector potential has to take into account all these components. Unfortunately they cannot be determined since several boundary conditions are still unknown due to their astrophysical origins. In addition, Eq. (8) shows that it is the net difference $\delta\mathbf{A} = \mathbf{A}_+ - \mathbf{A}_-$ between the vector potentials of the two branes that is relevant, not the local values on the branes. For all these reasons, the effective ambient magnetic vector potential $\delta\mathbf{A}_{amb}$ "could be very large... or null." To simplify, we consider hereafter $\delta\mathbf{A}_{amb}$ as an unknown parameter of the model. Nevertheless, to be consistent with
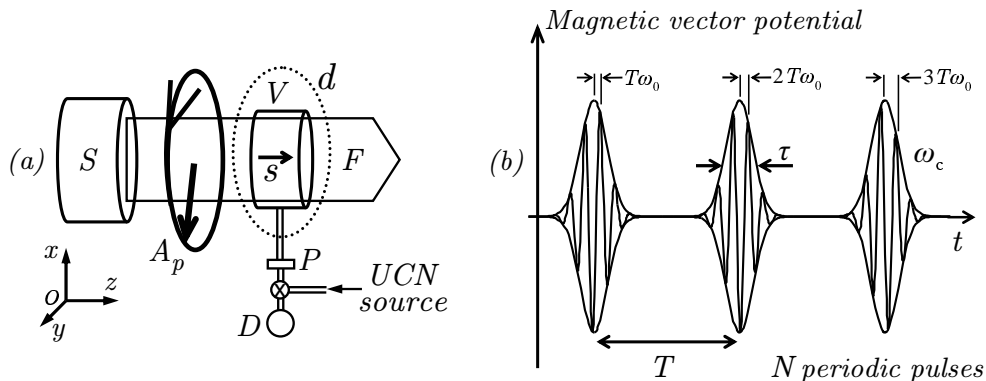
FIG. 2: Sketch of the experimental device for the study of particle swapping between branes. a: In a first step, the ultracold neutron gas is stored in the vessel (V) after neutrons have been polarized by the polarizer (P). Neutrons' spins (s) are polarized perpendicularly to the plane of rotation of $\mathbf{A}_p$. In a second step, the neutron gas is subjected to a pulsed electromagnetic beam (F) from a frequency comb source (S). After a run of excitations, the vessel is emptied and neutrons are counted with a detector (D). The device is completed by a neutron decay detector (d). b: Sketch of the amplitude of the magnetic vector potential related to the beam (F) against time t. The field is a set of N coherent pulses. T is the time period between each pulse while τ is the pulse duration. ω_c is the pulsation of the carrier wave while $T\omega_0$ denotes the dephasing between the carrier wave and the pulse maximum.

observations, Eq. (9) shows that any ambient magnetic vector potential $\delta\mathbf{A}_{amb}$ should be balanced by an ambient confining potential $\eta\hbar$, such that $\Omega_p/\eta \ll 1$ (in order to avoid unseen oscillations of "free" fermions).

Finally, since in the following one is seeking for a resonant oscillatory mechanism, a first requirement is to consider a rotating magnetic vector potential as explained before. Such a potential can obviously be obtained from a coherent electromagnetic wave with a circular polarization. In that case, the magnetic vector potential $\mathbf{A}$ is trivially related to the electric and magnetic fields through $\mathbf{E} = -\partial\mathbf{A}/\partial t$ and $\mathbf{B} = \nabla \times \mathbf{A}$.

IV.   SETUP FOR RESONANT NEUTRON SWAPPING BETWEEN BRANES

In the present section, we give a sketch of an experimental setup that might be suitable to investigate the resonant mechanism described in the previous section. Under a suitable rotative field $\mathbf{A}_p$, a neutron n may disappear from our brane to the other one, i.e. $n \to n'$ (where the "prime" denotes the neutron in the second brane), but for an observer in our brane we get $n \to nothing$ (Fig. 1). In the present experiment, we consider an ultracold neutron gas (i.e. neutrons with a kinetic energy around 100 neV) as justified in section III A.

In a Coulomb gauge, a rotative magnetic vector potential $\mathbf{A}_p$ can be obtained from a circularly polarized electromagnetic wave. However, to achieve the conditions of a successful matter exchange, one must deal with the following difficulties:

(i) The value of the coupling constant g likely results in hardly detectable effects. If the coupling constant g is small enough, the phenomenon will not be easily observed since the resonance width will then become narrower than the bandwidth of any available coherent sources. To achieve the conditions of a successful matter exchange, the applied electromagnetic waves must possess a bandwidth lower than the resonance width, as shown in section III. In Refs. [7–9], values such that $g \leq 10^3$ m^{-1} were usually considered, though it was shown that our model could be in agreement with known physics even for $g < 10^{10}$ m^{-1}[8]. However those values are very low and remain problematic in the present experimental context.

(ii) The unknown magnitude and time dependence of η make difficult or even preclude the observation of a resonant swapping at a fixed frequency.

To overcome these restrictions, a possibility is to consider the frequency comb technique introduced by Hänsch [14] and well known by spectroscopists [15–17]: excitation by a train of phase-coherent pulses allows us to reach narrow resonance bandwidths with a larger efficiency on a large wavelength domain. Such a frequency comb source can be produced by using mode-locked (phase-locked) lasers through the multiple reflections of a pulse inside an optical Fabry-Pérot cavity. Nevertheless, we do not describe or discuss here the detailed way to produce a frequency comb source, which has been widely described elsewhere by many other authors [14–17] and which is out of the scope of the present paper.

Let us now study the applicability of this technique to force the swapping of neutrons between the branes.

A. Source of excitation

Ultracold neutrons are stored in a convenient vessel (emptied of atmospheric gases) which is supplied with a train of N phase-coherent pulses related to an electromagnetic wave having a magnetic field amplitude B_0 (see Fig. 2). The magnetic vector potential felt by a neutron in the cavity can be expressed as [14]:

$$\mathbf{A}_p(t) = \frac{B_0 c}{\omega_c} \sum_{n=0}^{N-1} \Upsilon_\tau(t - nT)\mathbf{e}(t - nT_0) \tag{10}$$

where $\mathbf{e}(t) = (\cos \omega_c t, \sin \omega_c t, 0)$, and ω_c is the angular frequency of the carrier wave. $\Upsilon_\tau(t)$ is the envelope function of a pulse, with τ the temporal pulse-width (see Fig. 2.b). One considers a usual Gaussian pulse such that $\Upsilon_\tau(t) = \exp(-4(t/\tau)^2 \ln 2)$. T is the time period between each pulse (see Fig. 2.b) such that $T \gg \tau$. One defines the frequency of repetition $f_r = 1/T$, with $2\pi f_r \ll \omega_c$. T_0 allows a phase difference between the carrier wave and the pulse maximum, with $|T - T_0| \leq 2\pi/\omega_c$. The spectrum of the field is therefore given by

$$|\mathbf{A}_p(\omega)|^2 = \frac{B_0^2 c^2}{2\omega_c^2} \left\{ S(\omega + \omega_0)\overline{\Upsilon}_\tau^2(\omega + \omega_c) + S(\omega - \omega_0)\overline{\Upsilon}_\tau^2(\omega - \omega_c) \right\} \tag{11}$$

with

$$\overline{\Upsilon}_\tau(\omega) = \int \Upsilon_\tau(t)e^{i\omega t}dt = \frac{\tau\sqrt{\pi}}{2\sqrt{\ln 2}} \exp\left(-\frac{\omega^2 \tau^2}{16 \ln 2}\right) \tag{12}$$

and

$$S(\omega) = \left| \sum_{n=0}^{N-1} e^{i\omega T n} \right|^2 = \frac{\sin^2(\omega T N/2)}{\sin^2(\omega T/2)} \tag{13}$$

and where

$$\omega_0 = \omega_c \left(1 - \frac{T_0}{T}\right) \tag{14}$$

Such a spectrum is a frequency comb (see Fig. 3) made of narrow peaks located at $\omega_k = 2k\pi f_r + \omega_0$ ($k \in \mathbb{N}$) for $\omega > 0$ (or at $\omega_k = -2k\pi f_r - \omega_0$ ($k \in \mathbb{N}$) for $\omega < 0$). For these frequencies one gets $S(\omega_k) = N^2$. The available frequencies can be fine-tuned by adjusting ω_0 (or f_r). The width at half-height of each peak is $\delta\omega \sim 5.57 f_r/N$, such that the temporal coherence of each frequency rises as N increases. One defines the fineness $F = 2\pi f_r/\delta\omega \sim N$. The number Q of useful frequency peaks is given by the width at half-height $\Delta\omega$ of the squared Gaussian function, i.e. $\Delta\omega = 4\sqrt{2}\ln 2/\tau \sim 4/\tau$ and one gets $Q = \Delta\omega/(2\pi f_r) = (2/\pi)(T/\tau)$.

Since $\mathbf{E}_p = -\partial\mathbf{A}_p/\partial t$, it must be noticed that the electric field of the wave presents a different pulse shape from the magnetic vector potential: the wave spectra considered from the electric and vector potential fields point of view are related through $|\mathbf{E}_p(\omega)|^2 = \omega^2 |\mathbf{A}_p(\omega)|^2$. This point is important since the pulse shape control can be experimentally obtained by properly designing the electric field [22].

In the experiment, any neutron is also submitted to the magnetic field $\mathbf{B}_p = (1/c)\mathbf{e}_z \times \mathbf{E}_p$ of the electromagnetic wave such that we get:

$$\mathbf{B}_p(t) = B_0 \sum_{n=0}^{N-1} \Upsilon_\tau(t - nT)\mathbf{e}_m^{(n)}(t) \tag{15}$$

where $\mathbf{e}_m^{(n)}(t) = \mathbf{e}(t - nT_0) + u(t - nT)\, \mathbf{e}_z \times \mathbf{e}(t - nT_0)$ with $u(t) = 8t\ln 2/(\omega_c \tau^2)$ and $\mathbf{e}_z = (0, 0, 1)$.

B. Neutron dynamics

In the experiment, in addition to the magnetic vector potential $\mathbf{A}_p(t)$, neutrons are submitted to the ambient gravitational fields ($V_\pm$) and the magnetic field $\mathbf{B}_p(t)$ of the electromagnetic wave. For completeness, we should also consider an ambient magnetic vector potential $\delta\mathbf{A}_{amb} = \delta A_{amb}\mathbf{u}$, where $\mathbf{u} = (\sin\theta\cos\varphi, \sin\theta\sin\varphi, \cos\theta)$ in the
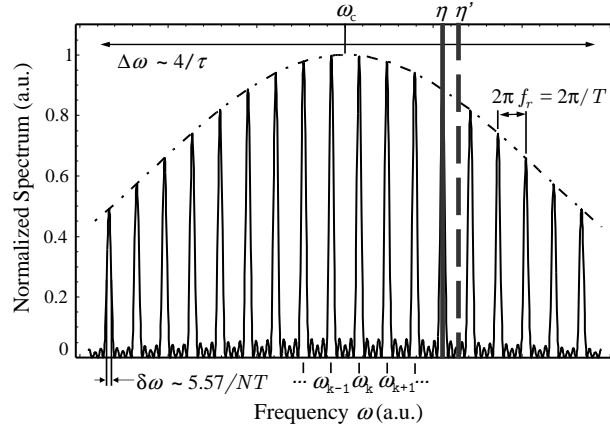
FIG. 3: Naive view of the frequency comb related to the spectrum of the pulsed coherent source. The full band (η) and the dashed band (η') correspond to two different possible values of the effective potential. The thickness of the bands is about $\delta\omega$ and corresponds to the width of the resonances. η' can shift towards η provided a suitable time variation of the potential. If the potential is not time-dependent, η' can match the frequency of a tooth of the comb provided that ω_0 is fine-tuned. The real number of teeth is many thousand times greater than on the present drawing.

system of reference $Oxyz$ (see Fig. 2.a). The low energy of neutrons in the vessel makes the nonrelativistic equations (5) to (8) valid. Therefore, from Eqs. (10) and (15), Eq. (5) can be expressed as

$$i\hbar\frac{\partial}{\partial t}\left|\Psi\right\rangle = \left\{\begin{bmatrix} V_+ & -iE_a\sigma\cdot\mathbf{u} \\ iE_a\sigma\cdot\mathbf{u} & V_- \end{bmatrix} + E_0\sum_{n=0}^{N-1}\Upsilon_\tau(t-nT)\times \right.$$
$$\left. \begin{bmatrix} \sigma\cdot\mathbf{e}_m^{(n)}(t) & -i\kappa\sigma\cdot\mathbf{e}(t-nT_0) \\ i\kappa\sigma\cdot\mathbf{e}(t-nT_0) & 0 \end{bmatrix}\right\}\left|\Psi\right\rangle \tag{16}$$

with $E_0 = (1/2)g_s\mu B_0$, $\kappa = gc/\omega_c$ and $E_a = (1/2)gg_s\mu\delta A_{amb}$.

According to Eq. (16), if $E_0 = E_a = 0$, in our brane, a neutron can be described by the eigenstates $\left|\psi_{\pm 1/2}^+\right\rangle$ with energy V_+ (the subscript "$\pm 1/2$" denotes both spin states along the Oz axis), whereas in the second brane, it will be described by the eigenstates $\left|\psi_{\pm 1/2}^-\right\rangle$ with energy V_-. In Eq. (16), it is then possible to write

$$\left|\Psi\right\rangle = a(t)e^{-i\hbar^{-1}V_+t}\left|\psi_{+1/2}^+\right\rangle + b(t)e^{-i\hbar^{-1}V_+t}\left|\psi_{-1/2}^+\right\rangle \tag{17}$$
$$+c(t)e^{-i\hbar^{-1}V_-t}\left|\psi_{+1/2}^-\right\rangle + d(t)e^{-i\hbar^{-1}V_-t}\left|\psi_{-1/2}^-\right\rangle$$

Substituting (17) into (16), the Pauli equation (16) reads:

$$\begin{cases} i\hbar\partial_t a(t) = E_0 b(t)e^{-i\omega_c t}(\Lambda(t)-i\widetilde{\Lambda}(t)) - i\kappa E_0 d(t)e^{i(\eta-\omega_c)t}\Lambda(t) - iE_a c(t)\cos\theta e^{i\eta t} - iE_a d(t)e^{-i\varphi}\sin\theta e^{i\eta t} \\ i\hbar\partial_t b(t) = E_0 a(t)e^{i\omega_c t}(\Lambda^*(t)+i\widetilde{\Lambda}^*(t)) - i\kappa E_0 c(t)e^{i(\eta+\omega_c)t}\Lambda^*(t) + iE_a d(t)\cos\theta e^{i\eta t} - iE_a c(t)e^{i\varphi}\sin\theta e^{i\eta t} \\ i\hbar\partial_t c(t) = i\kappa E_0 b(t)e^{-i(\eta+\omega_c)t}\Lambda(t) + iE_a a(t)\cos\theta e^{-i\eta t} + iE_a b(t)e^{-i\varphi}\sin\theta e^{-i\eta t} \\ i\hbar\partial_t d(t) = i\kappa E_0 a(t)e^{-i(\eta-\omega_c)t}\Lambda^*(t) - iE_a b(t)\cos\theta e^{-i\eta t} + iE_a a(t)e^{i\varphi}\sin\theta e^{-i\eta t} \end{cases} \tag{18}$$

with $\Lambda(t) = \sum_{n=0}^{N-1}\Upsilon_\tau(t-nT)e^{i\omega_c nT_0}$ and $\widetilde{\Lambda}(t) = \sum_{n=0}^{N-1}\Upsilon_\tau(t-nT)u(t-nT)e^{i\omega_c nT_0}$, and where "$*$" denotes the complex conjugate.

Eqs. (18) are complex to solve exactly without numerical computation. Nevertheless, the secular approximation and the first order perturbation theory can be applied to obtain an approximate solution of the system (18). In the following, we assume that ω_c has the same magnitude as $|\eta|$.

First, if $\kappa = 0$ and $E_a = 0$, from the first order perturbation theory it can be shown that the terms involving the function $\Lambda(t) - i\widetilde{\Lambda}(t)$ lead to an amplitude contribution equal to zero and can therefore be ignored in the whole system [23].

Next, it is worth remembering that Eq. (9) also implies $E_a/\hbar|\eta| \ll 1$ for consistency (to avoid undetected "free" oscillations of fermions, see section III B). Then, considering the secular approximation, the terms with $E_a\exp(\pm i\eta t)$

exhibiting rapid variations can be neglected. Indeed these terms lead to amplitude contributions $E_a/(\hbar\eta)$, which are then much smaller than 1. It must be pointed out that the influence of a hypothetic ambient magnetic vector potential vanishes in that case.

At last, if $\eta > 0$ (or $\eta < 0$), the terms with $\kappa E_0 \exp(\pm i(\eta + \omega_c)t)$ (or $\kappa E_0 \exp(\pm i(\eta - \omega_c)t)$) exhibit rapid variations since $|\eta + \omega_c| \gg |\eta - \omega_c|$ (or $|\eta - \omega_c| \gg |\eta + \omega_c|$). As a consequence, the secular approximation allows us to neglect the terms with $\exp(\pm i(\eta + \omega_c)t)$ if $\eta > 0$ (or the terms with $\exp(\pm i(\eta - \omega_c)t)$ if $\eta < 0$).

These simplifications allow us to rewrite the system (18) as two independent systems in a very compact form:

(i) If $\eta > 0$:

$$\left\{ \begin{array}{l} \partial_t a(t) = -\Omega_p e^{i(\eta - \omega_c)t}\Lambda(t)d(t) \\ \partial_t d(t) = \Omega_p e^{-i(\eta - \omega_c)t}\Lambda^*(t)a(t) \end{array} \right. \tag{19}$$

(ii) If $\eta < 0$:

$$\left\{ \begin{array}{l} \partial_t b(t) = -\Omega_p e^{i(\eta + \omega_c)t}\Lambda^*(t)c(t) \\ \partial_t c(t) = \Omega_p e^{-i(\eta + \omega_c)t}\Lambda(t)b(t) \end{array} \right. \tag{20}$$

with $\Omega_p = \kappa E_0/\hbar$. For a fixed circular polarization of the electromagnetic wave, the two systems (19) and (20) introduce a constraint on the spin state in which the neutron must be prepared to allow the swapping. Since the influence of the electromagnetic wave can be treated as a simple perturbation, the systems (19) and (20) can be solved analytically by using first order perturbation theory. For a neutron initially localized in our brane at time $t = 0$, and prepared with an initial spin state $s = \pm 1/2$ (in relation to $\eta = \pm|\eta|$), the probability $P_{\pm 1/2}$ to find the particle in the second brane is finally:

$$P_{\pm 1/2} = \Omega_p^2 \overline{\Upsilon}_\tau^2(\omega_c \mp \eta)S(\eta \mp \omega_0) \tag{21}$$

with $S(\eta \mp \omega_0) = S(\omega = \eta \mp \omega_0)$ (see Eq. (13)). According to Eqs. (11), (12) and (13), Eqs. (19) to (21) show that a resonant swapping occurs when the frequency $\omega_k = 2k\pi f_r \pm \omega_0$ of the frequency comb matches η. In addition, the width at half-height of each resonance is $\delta\omega \sim 5.57 f_r/N$, i.e. corresponds to the width of a tooth of the comb (Fig. 3). Assuming that the frequency of resonance is achieved in the domain of frequencies covered by the comb, one gets:

$$P_{\pm 1/2} \sim \tau^2 \Omega_p^2 N^2 \tag{22}$$

As shown by Hänsch for spectroscopy [14], the probability $P_{\pm 1/2}$ increases as the square of N increases; i.e. the probability increases as the teeth of the frequency comb become narrower. In addition, the use of a frequency comb technique allows us then to achieve intense pulsed fields enhancing Ω_p and thus $P_{\pm 1/2}$. Indeed, the pulsed mode permits intense electromagnetic fields and therefore large values of A_p. For instance, common pulsed sources can easily reach intensities of 10^{14} W·cm^{-2} up to 10^{18} W·cm^{-2} [24]. Since $\Omega_p = g g_s \mu A_p/(2\hbar)$, one can increase the coupling and $P_{\pm 1/2}$ despite the weak value of g. The frequency comb seems therefore to be a better candidate than any other electromagnetic field configuration for achieving conditions of a successful matter swapping between branes.

Now, since the excitation time t_e during which neutrons feel a set of coherent pulses is $t_e \sim NT$, the rate Γ of neutron exchange between branes is simply (at resonance):

$$\Gamma = P_{\pm 1/2}/t_e = \tau^2 \Omega_p^2 N/T \tag{23}$$

C. Experimental consequences and discussion

(1) **Neutron gas polarization**.

According to Eqs. (19) and (20), a neutron initially in a spin-up state in our brane reaches the other brane in a spin-down state (and reciprocally). Therefore, in order to achieve a successful transfer, the neutron gas in the vessel must be polarized before the experiment with a direction of polarization normal to the plane of rotation of the magnetic vector potential of the incident electromagnetic wave (Fig. 2.a). It appears that the collisional dynamics between neutrons or in relation with the storage chamber walls is negligible provided that collisional time t_c is greater than t_e which is assumed to be satisfied in the experimental conditions. Moreover since the neutron gas is polarized, the Pauli exclusion principle will favor an increase of the collisional time t_c thus promoting the experimental success.

(2) **Measure of the rate of neutron exchange**.

Let N_0 be the initial number of neutrons in the storage chamber. Γ_n is the loss rate of neutrons that takes into account the usual decay rate and the losses in the vessel (in the following, one only uses the usual decay rate value
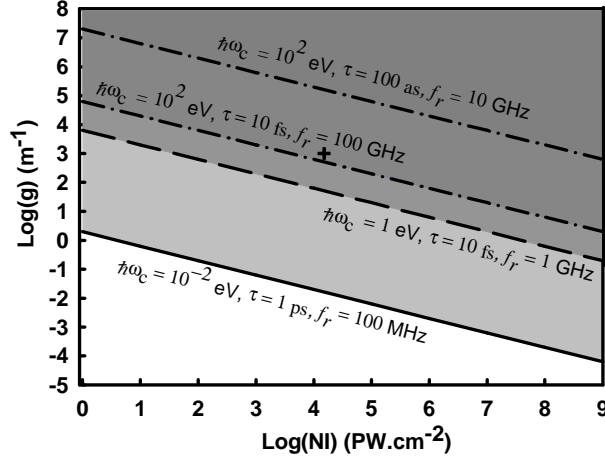
FIG. 4: Values of the coupling constant g leading to an observable swapping of neutrons between two branes. The values of g are given against the effective pulsed beam intensity NI. Each line is the lower reachable limit, defined by $\Gamma = 0.1\Gamma_n$, for some specific carrier wave pulsation ω_c, pulse duration τ, and frequency repetition f_r. Grey areas up to a given line correspond to $\Gamma \geq 0.1\Gamma_n$.

for computations). t_s is the storage time (i.e. the duration of an experiment). In a first calibration experiment, $N_c(t_s) = N_0 \exp(-\Gamma_n t_s)$ will be the number of remaining neutrons in the vessel after an experimental run without an applied electromagnetic field. In a second experiment where the wave is switched on, the number of recorded neutrons will be then given by: $N_{c,f}(t_s) = N_0 \exp(-\Gamma t_s)\exp(-\Gamma_n t_s)$. Then, the neutron transfer between branes could be simply detected by measuring the ratio: $N_{c,f}(t_s)/N_c(t_s) = \exp(-\Gamma t_s)$. The number of stored neutrons, before and after electromagnetic field switching, can be directly counted (see Fig. 2.a) by a helium-3 neutron detector for instance (see Baker *et al* [10]).

According to the duration of the experiment, it can be relevant to also measure the neutron decays. In a first calibration experiment, $N_c^{(d)}(t) = N_0(1 - \exp(-\Gamma_n t))$ will be then the number of usual neutron decays during an experimental run without the electromagnetic field. In a second experiment where the wave is switched on, the number of recorded events will be then given by: $N_{c,f}^{(d)}(t) = N_0(\Gamma_n/(\Gamma_n + \Gamma)) \cdot (1 - \exp(-(\Gamma_n + \Gamma)t))$. Then, the neutron transfer between branes could be simply described through the ratio: $(dN_{c,f}^{(d)}(t)/dt)/(dN_c^{(d)}(t)/dt) = \exp(-\Gamma t)$.

According to some previous experimental results about ultracold neutrons [10–13], a relevant criterion to clearly prove the effect is to achieve $\Gamma \sim 0.1\Gamma_n$ at least. As a consequence, it is possible to define the sensitivity of the experiment. Using $E_c = \hbar\omega_c$ and $f_r = 1/T$, one can write Eq. (23) as:

$$\Gamma = K \frac{f_r \tau^2 NI}{E_c^2} g^2 \tag{24}$$

where I is the intensity of the pulse. In the above expression, E_c is given in eV, f_r in GHz, I in PW·cm^{-2}, τ in fs, and $K = g_s^2\mu^2/(200c\varepsilon_0 e^2) \sim 2.74 \cdot 10^{-14}$ (in the relevant units). Figure 4 plots the value of the coupling constant leading to an observable effect. The values of g are given against the effective pulsed beam intensity NI. Each line is the lower reachable limit (such that $\Gamma = 0.1\Gamma_n$) for some specific conditions (see Fig. 4).

(3) Conditions of resonance.

Let us now discuss how to deal with the unknown value of η and its time dependence. The frequency comb source yields simultaneously a set of frequencies covering a large frequency domain around the frequency of the carrier wave (Fig. 3). Usual frequency combs can offer a number of useful frequencies such that $Q \sim 10^5 - 10^6$ [15–17]. As a consequence, for a large frequency domain, one can simultaneously probe up to a million of frequencies since neutrons feel them all together. As detailed hereafter, this is a very efficient way to achieve the resonance without knowledge of the value of η, provided it is located in the comb width (see Fig. 3). Of course, as previously suggested, η can reach many possible values in different domains of the electromagnetic spectrum. As a consequence, in order to increase the chance of success of such an experiment it could be highly beneficial to consider different frequency comb sources such as terahertz lasers [16], vacuum and extreme ultraviolet lasers [17], or free-electron lasers in X-rays domain [25]. With some distinct frequency combs, one can then expect to quickly cover the most relevant frequency domains of the electromagnetic spectrum.

As an illustration, let us consider the case $E_c = 1$ eV, $\tau = 10$ fs, $f_r = 1$ GHz and $g = 10^3$ m^{-1} (see Fig. 4). We suppose that $I = 5 \cdot 10^{16}$ W·cm^{-2} and $N = 300$ (see cross in Fig. 4). This leads to a comb with $Q \sim 6.4 \cdot 10^4$ frequencies. The resonance width is $\delta\omega \sim 18.6$ Mrad·s^{-1}. With the values mentioned, we get $\Gamma \sim 4.11 \cdot 10^{-2}$ s^{-1}. With such a value, after a delay of about 2.6 s, a population of neutrons is reduced from 10 %. Two cases could then be considered:

(i) η is not time-dependent.

If required, each frequency between two teeth of the comb can be scanned by varying ω_0 shifting then the frequency ω_k of each tooth. Since the resonance width is given by $\delta\omega$, the number of frequencies to be scanned between two teeth is given by the fineness $F = 2\pi f_r/\delta\omega \sim N$. As a consequence, on the whole frequency domain covered by the comb, one can probe NQ frequencies just with N experimental runs (usually N can vary from 10 to 10000). In the present illustration, $NQ \sim 1.9 \cdot 10^7$ frequencies can be explored. Spending 2.6 s on a given set of Q frequencies, for $N = 300$, the whole experiment takes $t_s = 13$ min to explore the NQ frequencies. Since we ignore the right domain of frequencies where η locates, in a first approach, it is not necessary to measure the number of neutrons in the vessel for each set of Q frequencies.

(ii) η is time-dependent.

Considering the time variation of η, we have explained that the time rate of shift for η is likely very small (see section III A). It means that η can spontaneously "scan" the frequency comb without a change of ω_0. This would allow circumventing the problem of time dependence of η since a resonant frequency will be always available provided that η is located into the comb width: a resonance occurs each time that η matches a frequency of a tooth of the comb. Using the time rate of shift of η of 1.7 meV/day, i.e. about 30 Mrad·s^{-1}/s (see section III A), each resonance is kept during 0.62 s since $\delta\omega \sim 18.6$ Mrad·s^{-1}. For an effective resonance maintained during 2.6 s, the resonance frequency must scan 5 teeth of the comb at least. Because of the frequency of repetition f_r, it needs 210 s to reach the next teeth of the comb, and thus $t_s = 14$ min are necessary to scan the five teeth.

In both cases, after an experimental run, about 10 % of the neutrons could be transferred to the other brane while about 60 % of the neutrons have disappeared due to the natural neutron decay. The quantity of neutrons remaining in the vessel can then be counted while the number of neutron decays is measured during the experimental run. It is worth noticing that during the whole experiment, provided that η is located on the comb width, the resonance condition is necessarily encountered one time (if η is not time-dependent, when the correct frequency tooth is crossed) or many times (if η is time-dependent, for each crossed tooth).

One notes that depending on the parameters (g, ω_c, I, N, ...) the required delay of the experiment can be characterized by longer time ($t_s \geq 15$ min) or shorter time of storage ($t_s \leq 15$ min) than in the previous example. In these cases, it could be more relevant to measure the decay of neutrons (long time of storage) instead of counting them (short time of storage), although both methods could be used together. At last, of course, in order to improve the accuracy of the results, it would be necessary to repeat the same experiment many times. For $t_s \sim 15$ min, even if the experiment is repeated 100 times for instance, a full experimental work takes about only 1 day. This makes supposed that our present experimental framework would lead to fair durations. In return, though our method allows one to easily achieve the resonance, one notes that it does not allow one to find the value η but instead a domain of values that corresponds to the width of the frequency comb (though a dichotomic search using combs with different widths could allow us to specify the value η).

V. CONCLUSION

Recent theoretical results have suggested the possibility of matter swapping between branes [7–9]. In the present work, a new experimental framework has been proposed to demonstrate this mechanism at a laboratory scale. The experiment, involving a resonant mechanism, uses an ultracold and polarized neutron gas interacting with a fine-tuned electromagnetic pulsed radiation. This experiment relies on the Hänsch frequency comb technique, commonly used in spectroscopy to overcome the limitations of the large bandwidth of electromagnetic sources [14–17]. The recorded experimental data are simply the rates at which particle exchange occurs between branes. Any success in this experiment would imply major consequences extending far beyond the demonstration of the existence of other branes. Moreover, the relative simplicity of the suggested setup is of considerable interest: existing devices used in spectroscopy [14–17, 25] and neutron physics investigations (neutron electric dipole moment [10], Lorentz invariance [11], neutron-mirror neutron oscillations [12] and coupling to axionlike particles [13] for instance) could possibly match the requirements of a successful experiment. Thus the present work takes place in a relevant current trend in

experimental works for new physics searches at a low energy scale [6, 10–13, 26].

[1] K. Akama, *Pregeometry*, Lect. Notes Phys. **176**, 267 (1983), arXiv:hep-th/0001113;
V.A. Rubakov, M.E. Shaposhnikov, *Do we live inside a domain wall?*, Phys. Lett. **125B**, 136 (1983);
M. Pavsic, *Einstein's gravity from a first order lagrangian in an embedding space*, Phys. Lett. **116A**, 1 (1986), arXiv:gr-qc/0101075;
P. Horava, E. Witten, *Heterotic and Type I String Dynamics from Eleven Dimensions*, Nucl. Phys. **B460**, 506 (1996), arXiv:hep-th/9510209;
A. Lukas, B.A. Ovrut, K.S. Stelle, D. Waldram, *The Universe as a Domain Wall*, Phys. Rev. D **59**, 086001 (1999), arXiv:hep-th/9803235;
L. Randall, R. Sundrum, *An alternative to compactification*, Phys. Rev. Lett. **83**, 4690 (1999), arXiv:hep-th/9906064;
J. Khoury, B.A. Ovrut, P.J. Steinhardt, N. Turok , *The Ekpyrotic Universe: Colliding Branes and the Origin of the Hot Big Bang*, Phys. Rev. D **64**, 123522 (2001) , arXiv:hep-th/0103239;
R. Davies, D. P. George, R. R. Volkas, *The standard model on a domain-wall brane?*, Phys. Rev. D **77**, 124038 (2008), arXiv:0705.1584 [hep-ph];
Y.-X. Liu, L.-D. Zhang, L.-J. Zhang, Y.-S. Duan, *Fermions on thick branes in the background of sine-Gordon kinks*, Phys. Rev. D **78**, 065025 (2008), arXiv:0804.4553 [hep-th].
[2] G. Dvali, G. Gabadadze, M. Shifman, *(Quasi)Localized Gauge Field on a Brane: Dissipating Cosmic Radiation to Extra Dimensions?*, Phys. Lett. B **497**, 271 (2001), arXiv:hep-th/0010071;
G. Dvali, G. Gabadadze, M. Porrati, *4D Gravity on a Brane in 5D Minkowski Space*, Phys. Lett. B **485**, 208 (2000), arXiv:hep-th/0005016.
[3] N. Arkani-Hamed, S. Dimopoulos, G. Dvali, N. Kaloper, *Manyfold Universe*, J. High Energy Phys. **12** (2000) 010, arXiv:hep-ph/9911386.
[4] L. Randall, R. Sundrum, *Large mass hierarchy from a small extra dimension*, Phys. Rev. Lett. **83**, 3370 (1999), arXiv:hep-ph/9905221.
[5] D. Hooper, S. Profumo, *Dark Matter and Collider Phenomenology of Universal Extra Dimensions*, Phys. Rep. **453**, 29 (2007), arXiv:hep-ph/0701197;
I. Antoniadis, N. Arkani-Hamed, S. Dimopoulos, G. Dvali, *New dimensions at a millimeter to a Fermi and superstrings at a TeV*, Phys. Lett. B **436**, 257 (1998), arXiv:hep-ph/9804398.
[6] J. Chiaverini, S. J. Smullin, A. A. Geraci, D. M. Weld, A. Kapitulnik, *New Experimental Constraints on Non-Newtonian Forces below 100 microns*, Phys. Rev. Lett. **90**, 151101 (2003), arXiv:hep-ph/0209325;
Y. Shtanov, A. Viznyuk, *Linearized gravity on the Randall-Sundrum two-brane background with curvature terms in the action for the branes*, Classical Quantum Gravity **22**, 987 (2005), arXiv:hep-th/0312261.
[7] M. Sarrazin, F. Petit, *Equivalence between domain walls and "noncommutative" two-sheeted spacetimes: Model-independent matter swapping between branes*, Phys. Rev. D **81**, 035014 (2010), arXiv:0903.2498 [hep-th].
[8] F. Petit, M. Sarrazin, *Quantum dynamics of massive particles in a non-commutative two-sheeted space-time*, Phys. Lett. B **612**, 105 (2005), arXiv:hep-th/0409084;
M. Sarrazin, F. Petit, *Quantum dynamics of particles in a discrete two-branes world model: Can matter particles exchange occur between branes?*, Acta Phys. Polon. B **36**, 1933 (2005), arXiv:hep-th/0409083.
[9] M. Sarrazin, F. Petit, *Matter localization and resonant deconfinement in a two-sheeted spacetime*, Int. J. Mod. Phys. A **22**, 2629 (2007), arXiv:hep-th/0603194.
[10] I. Altarev, C. A. Baker, G. Ban, K. Bodek, M. Daum, M. Fertl, B. Franke, P. Fierlinger, P. Geltenbort, K. Green, M. G. D. van der Grinten, P. G. Harris, R. Henneck, M. Horras, P. Iaydjiev, S. N. Ivanov, N. Khomutov, K. Kirch, S. Kistryn, A. Knecht, A. Kozela, F. Kuchler, B. Lauss, T. Lefort, Y. Lemière, A. Mtchedlishvili, O. Naviliat-Cuncic, J. M. Pendlebury, G. Petzoldt, E. Pierre, F. M. Piegsa, G. Pignol, G. Quéméner, D. Rebreyend, S. Roccia, P. Schmidt-Wellenburg, N. Severijns, D. Shiers, K. F. Smith, Yu. Sobolev, J. Zejma, J. Zenner, G. Zsigmond, *New constraints on Lorentz invariance violation from the neutron electric dipole moment*, Europhys. Lett. **92**, 51001 (2010), arXiv:1006.4967 [nucl-ex];
C. A. Baker, D.D. Doyle, P. Geltenbort, K. Green, M.G.D. van der Grinten, P.G. Harris, P. Iaydjiev, S.N. Ivanov, D. J. R. May, J.M. Pendlebury, J.D. Richardson, D. Shiers, K.F. Smith, *Improved Experimental Limit on the Electric Dipole Moment of the Neutron*, Phys. Rev. Lett. **97**, 131801 (2006), arXiv:hep-ex/0602020.
[11] I. Altarev, C. A. Baker, G. Ban, G. Bison, K. Bodek, M. Daum, P. Fierlinger, P. Geltenbort, K. Green, M. G. D. van der Grinten, E. Gutsmiedl, P. G. Harris, W. Heil, R. Henneck, M. Horras, P. Iaydjiev, S. N. Ivanov, N. Khomutov, K. Kirch, S. Kistryn, A. Knecht, P. Knowles, A. Kozela, F. Kuchler, M. Kuz'niak, T. Lauer, B. Lauss, T. Lefort, A. Mtchedlishvili, O. Naviliat-Cuncic, A. Pazgalev, J. M. Pendlebury, G. Petzoldt, E. Pierre, G. Pignol, G. Quéméner, M. Rebetez, D. Rebreyend, S. Roccia, G. Rogel, N. Severijns, D. Shiers, Yu. Sobolev, A. Weis, J. Zejma, G. Zsigmond,*Test of Lorentz Invariance with Spin Precession of Ultracold Neutrons*, Phys. Rev. Lett. **103**, 081602 (2009), arXiv:0905.3221 [nucl-ex].
[12] I. Altarev, C. A. Baker, G. Ban, K. Bodek, M. Daum, P. Fierlinger, P. Geltenbort, K. Green, M. G. D. van der Grinten, E. Gutsmiedl, P. G. Harris, R. Henneck, M. Horras, P. Iaydjiev, S. Ivanov, N. Khomutov, K. Kirch, S. Kistryn, A. Knecht, P. Knowles, A. Kozela, F. Kuchler, M. Kuz'niak, T. Lauer, B. Lauss, T. Lefort, A. Mtchedlishvili, O. Naviliat-Cuncic, S. Paul, A. Pazgalev, J. M. Pendlebury, G. Petzoldt, E. Pierre, C. Plonka-Spehr, G. Quéméner, D. Rebreyend, S. Roccia, G. Rogel,

N. Severijns, D. Shiers, Yu. Sobolev, R. Stoepler, A. Weis, J. Zejma, J. Zenner, G. Zsigmond,*Neutron to Mirror-Neutron Oscillations in the Presence of Mirror Magnetic Fields*, Phys. Rev. D **80**, 032003 (2009), arXiv:0905.4208 [nucl-ex];

A.P. Serebrov, E.B. Aleksandrov, N.A. Dovator, S.P. Dmitriev, A.K. Fomin, P. Geltenbort, A.G. Kharitonov, I.A. Krasnoschekova, M.S. Lasakov, A.N. Murashkin, G.E. Shmelev, V.E. Varlamov, A.V. Vassiljev, O.M. Zherebtsov, O.Zimmer, *Search for neutron-mirror neutron oscillations in a laboratory experiment with ultracold neutrons*, Nucl. Instrum. Meth. A **611**, 137 (2009), arXiv:0809.4902 [nucl-ex];

A.P. Serebrov, E.B. Aleksandrov, N.A. Dovator, S.P. Dmitriev, A.K. Fomin, P. Geltenbort, A.G. Kharitonov, I.A. Krasnoschekova, M.S. Lasakov, A.N. Murashkin, G.E. Shmelev, V.E. Varlamov, A.V. Vassiljev, O.M. Zherebtsov, O. Zimmer, *Experimental search for neutron - mirror neutron oscillations using storage of ultracold neutrons*, Phys. Lett. B **663**, 181 (2008), arXiv:0706.3600 [nucl-ex];

G. Ban, K. Bodek, M. Daum, R. Henneck, S. Heule, M. Kasprzak, N. Khomutov, K. Kirch, S. Kistryn, A. Knecht, P. Knowles, M. Kuzniak, T. Lefort, A. Mtchedlishvili, O. Naviliat-Cuncic, C. Plonka, G. Quéméner, M. Rebetez, D. Rebreyend, S. Roccia, G. Rogel, M. Tur, A. Weis, J. Zejma, G. Zsigmond , *Direct Experimental Limit on Neutron Mirror-Neutron Oscillations*, Phys. Rev. Lett. **99**, 161603 (2007), arXiv:0705.2336 [nucl-ex].

[13] S. Baessler, V.V. Nesvizhevsky, K.V. Protasov, A.Yu. Voronin, *Constraint on the coupling of axionlike particles to matter via an ultracold neutron gravitational experiment*, Phys. Rev. D **75**, 075006 (2007), arXiv:hep-ph/0610339.

[14] R. Teets, J. Eckstein, T.W. Hänsch, *Coherent two-photon excitation by multiple light pulses*, Phys. Rev. Lett. **38**, 760 (1977);

J.N. Eckstein, A.I. Ferguson, T.W. Hänsch, *High-Resolution Two-Photon Spectroscopy with Picosecond Light Pulses*, Phys. Rev. Lett. **40**, 847 (1978).

[15] T.M. Fortier, Y. Le Coq, J. E. Stalnaker, D. Ortega, S. A. Diddams, C. W. Oates, L. Hollberg, *Kilohertz-Resolution Spectroscopy of Cold Atoms with an Optical Frequency Comb*, Phys. Rev. Lett. **97**, 163905 (2006), arXiv:physics/0605034;

M.J. Thorpe, J. Ye, *Cavity-enhanced direct frequency comb spectroscopy*, Appl. Phys. B **91**, 397 (2008).

[16] T. Yasui, S. Yokoyama, H. Inaba, K. Minoshima, T. Nagatsuma, T. Araki,*Terahertz Frequency Metrology Based on Frequency Comb*, IEEE Journal of Selected Topics in Quantum Electronics **99**, 1 (2010);

T. Yasui, Y. Kabetani, E. Saneyoshi, S. Yokoyama, T. Araki, *Terahertz frequency comb by multifrequency-heterodyning photoconductive detection for high-accuracy, high-resolution terahertz spectroscopy* , Appl. Phys. Lett. **88**, 241104 (2006);

Y.-S. Juan, F.-Y. Lin, *Microwave-frequency-comb generation utilizing a semiconductor laser subject to optical pulse injection from an optoelectronic feedback laser*, Opt. Lett. **34**, 1636 (2009).

[17] D.Z. Kandula, C. Gohle, T.J. Pinkert, W. Ubachs, K.S.E. Eikema, *Extreme Ultraviolet Frequency Comb Metrology*, Phys. Rev. Lett. **105**, 063001 (2010);

D.C. Yost, T.R. Schibli, J. Ye, J.L. Tate, J. Hostetter, M.B. Gaarde, K.J. Schafer, *Vacuum-ultraviolet frequency combs from below-threshold harmonics*, Nature Physics **5**, 815 (2009);

R.J. Jones, K.D. Moll, M.J. Thorpe, J. Ye, *Phase-Coherent Frequency Combs in the Vacuum Ultraviolet via High-Harmonic Generation inside a Femtosecond Enhancement Cavity*, Phys. Rev. Lett. **94**, 193201 (2005).

[18] The gauge field is localized on each domain wall through a Dvali-Gabadadze-Porrati-Shifman mechanism [2].

[19] A. Connes, J. Lott, *Particle models and non-commutative geometry*, Nucl. Phys. B, Proc. Suppl. **18**, 29 (1991);

N.A. Viet, K.C. Wali, *Non-commutative geometry and a Discretized Version of Kaluza-Klein theory with a finite field content*, Int. J. Mod. Phys. A **11**, 533 (1996), arXiv:hep-th/9412220.

[20] S. Abel and B. Schofield, *Brane-Antibrane Kinetic Mixing, Millicharged Particles and SUSY Breaking*, Nucl. Phys. **B685**, 150 (2004), arXiv:hep-th/0311051;

R. Foot, A. Yu. Ignatiev, R.R. Volkas, *Physics of mirror photons*, Phys. Lett. B **503**, 355 (2001), arXiv:astro-ph/0011156.

[21] R. Lakes, *Experimental Limits on the Photon Mass and Cosmic Magnetic Vector Potential*, Phys. Rev. Lett. **80**, 1826 (1998);

J. Luo, C.-G. Shao, Z.-Z. Liu, Z.-K. Hu, *Determination of the limit of photon mass and cosmic magnetic vector with rotating torsion balance*, Phys. Lett. A **270**, 288 (2000);

A.S. Goldhaber, M.M. Nieto, *Problems of the rotating-torsion-balance limit on the photon mass*, Phys. Rev. Lett. **91**, 149101 (2003), arXiv:hep-ph/0305241.

[22] C.-B. Huang, Z. Jiang, D.E. Leaird, J. Caraquitena, A.M. Weiner, *Spectral line-by-line shaping for optical and microwave arbitrary waveform generations*, Laser & Photon. Rev. **2**, 227 (2008);

V.R. Supradeepa, C.-B. Huang, D.E. Leaird, A.M. Weiner, *Femtosecond pulse shaping in two dimensions: Towards higher complexity optical waveforms*, Opt. Express **16**, 11878 (2008);

J.W. Wilson, P. Schlup, R.A. Bartels, *Ultrafast phase and amplitude pulse shaping with a single, one-dimensional, high-resolution phase mask*, Opt. Express **15**, 8979 (2007).

[23] One notes that a magnetic field which would be described by a function similar to Eq. (10) does not give a null contribution. In addition, it could be shown that such a magnetic field would not correspond to a relevant magnetic vector potential. By contrast, the magnetic vector potential here used (Eq. (10)) gives a magnetic field (Eq. (15)) that allows a compensation mechanism that avoids a spin depolarization between each pulse whatever the laser intensity. As a consequence, the pulse design must be considered carefully in the experiment [22].

[24] M.P. Kalashnikov, P.V. Nickles, Th. Schlegel, M. Schnuerer, F. Billhardt, I. Will, W. Sandner, N.N. Demchenko, *Dynamics of Laser-Plasma Interaction at 10^{18} W/cm^2*, Phys. Rev. Lett. **73**, 260 (1994);

L.M. Gorbunov, S. Yu. Kalmykov, P. Mora, *Laser wakefield acceleration by petawatt ultra-short laser pulses*, Phys. Plasmas **12**, 033101 (2005), arXiv:physics/0409138.

[25] Z. Huang, K.-J. Kim, *Review of X-ray free-electron laser theory*, Phys. Rev. ST Accel. Beams **10**, 034801 (2007);

Z. Huang, R.D. Ruth, *Fully Coherent X-ray Pulses from a Regenerative Amplifier Free Electron Laser*, Phys. Rev. Lett. **96**, 144801 (2006); F. Grüner, S. Becker, U. Schramm, T. Eichner, R. Weingartner, D. Habs, J. Meyer-ter-Vehn, M. Geissler, M. Ferrario, L. Serafini, B. van der Geer, H. Backe, W. Lauth, S. Reiche, *Design considerations for table-top, laser-based VUV and X-ray free electron lasers*, Appl. Phys. B **86**, 431 (2007).

[26] M. Ahlers, H. Gies, J. Jaeckel, J. Redondo, A. Ringwald, *Laser experiments explore the hidden sector*, Phys. Rev. D **77**, 095001 (2008), arXiv:0711.4991 [hep-ph];
S.N. Gninenko, N.V. Krasnikov, A. Rubbia, *Extra dimensions and invisible decay of orthopositronium*, Phys. Rev. D **67**, 075012 (2003), arXiv:hep-ph/0302205.